

New Iron-Containing Electrode Materials for Lithium Secondary Batteries

Young-Sik Hong, Kwang Sun Ryu, and Soon Ho Chang

Using a galvanostatic charge/discharge cyler and cyclic voltammetry, we investigated for the first time the electrochemical properties of iron-containing minerals, such as chalcophanite, diadochite, schwertmannite, laihuite, and tinticite, as electrode materials for lithium secondary batteries. Lithium insertion into the mineral diadochite showed a first discharge capacity of about 126 mAh/g at an average voltage of 3.0 V vs. Li/Li⁺, accompanied by a reversible capacity of 110 mAh/g at the 60th cycle. When the cutoff potential was down to 1.25 V, the iron was further reduced, giving rise to a new plateau at 1.3 V. Although the others showed discharge plateaus at low potentials of less than 1.6 V, these results give an important clue for the development of new electrode materials.

Keywords: Lithium battery, cathode, mineral, diadochite.

I. Introduction

The explosive demand for portable electronic devices has increased the importance of compact, lightweight, and reliable lithium secondary batteries, which consist of a transition metal oxide cathode and a graphite anode. The graphite anode commonly used in lithium secondary batteries has a limited gravimetric capacity of 372 mAh/g and poses some safety risks. This prompted researchers to stabilize the electrochemical performance of the carbonaceous anode materials or to find alternatives. The latter has consequently led to the discovery of new anode materials with large capacities, such as vanadates [1], amorphous tin composite oxides [2], metal alloys [3], and nitrides [4]. Although a large irreversible capacity loss during the 1st cycle makes them less technologically interesting, the development of non-carbonaceous anode materials is being extensively pursued [5].

In line with this, one group investigated new cathode materials with framework structures containing polyanions, such as sulfates, phosphates, and arsenates, particularly, olivine-structured LiFePO₄ [6]. One of the most encouraging advantages of LiFePO₄ is that it discharges at 3.4 V vs. Li/Li⁺, it cycles well at an ambient temperature, and it has a reversible capacity of about 140–150 mAh/g. The energy state of the Fe³⁺/Fe²⁺ redox couple depends on its crystal structure and bonding character resulting from an electrostatic field of Fe³⁺/Fe²⁺ and a covalency of Fe³⁺/Fe²⁺-O bonding [6], [7]. LiFePO₄ is a well-known mineral and available in nature, which means it is neither scarce nor expensive [8]. In this respect, minerals containing electrochemically active species also provide an attractive area of new electrode materials. In fact, many geologists have already accumulated a large number of databases on minerals over a long time. Therefore, it is

Manuscript received December 17, 2002; revised July 2, 2003.

This work was supported by the Ministry of Information and Communication of Korea.

Young-Sik Hong (phone: +82 42 860 5057, email: youngsik@etri.re.kr), Kwang Sun Ryu (email: ryuks@etri.re.kr), and Soon Ho Chang (email: shochang@etri.re.kr) are with Basic Research Laboratory, ETRI, Daejeon, Korea.

interesting to investigate the electrochemical properties of iron-containing minerals because of their low price and abundance. To be sure, we searched a large number of iron-containing minerals and found some candidates, which are listed in Table 1. According to the theoretical capacities based on the $\text{Fe}^{3+}/\text{Fe}^{2+}$ redox couple, it is possible to find high-capacity electrode materials, such as avasite. Among them, two papers recently reported on the electrochemical properties of giniite and phosphosiderite [9], [10]. We cannot theoretically predict reactivity between minerals and lithium ions, but minerals with a high ratio of iron are suitable for high capacity electrode applications, e.g., Fe_3PO_7 and Fe_3BO_6 [$\text{Fe}/\text{P}(\text{B}) = 3$] [11]-[13].

In this paper, we report on the electrochemical properties of five minerals from different mining locations as an electrode material for lithium secondary batteries. Since the mineral diadochite discharged at 3.0 V, we focused on it as a cathode candidate in more detail.

Table 1. List of Fe^{3+} -containing minerals.

Mineral name	Chemical formula	Theoretical capacity (mAh/g)
Angelellite	$\text{Fe}_4\text{As}_2\text{O}_{11}$	195
Apatelite*	$\text{Fe}_3(\text{SO}_4)_2(\text{OH})_5 \cdot 0.5\text{H}_2\text{O}$	181
Avasite*	$5\text{Fe}_2\text{O}_3 \cdot 2\text{SiO}_2 \cdot 9\text{H}_2\text{O}$	292
Azovskite	$\text{Fe}_3(\text{PO}_4)(\text{OH})_6$	221
Chalcophanite ⁺	$(\text{Zn},\text{Fe},\text{Mn})\text{Mn}_3\text{O}_7 \cdot 3\text{H}_2\text{O}$?
Diadochite*	$\text{Fe}_2(\text{PO}_4)(\text{SO}_4)(\text{OH}) \cdot 5\text{H}_2\text{O}$	168
Giniite*	$\text{Fe}_2+\text{Fe}_4(\text{PO}_4)_3(\text{OH})_5 \cdot 2\text{H}_2\text{O}$	166
Laihuite	$\text{Fe}_3\text{Si}_2\text{O}_8$	229
Meurigite*	$\text{KFe}_7(\text{PO}_4)_5(\text{OH})_7 \cdot 8\text{H}_2\text{O}$	183
Phosphosiderite*	$\text{FePO}_4 \cdot 2\text{H}_2\text{O}$	178
Schwertmannite	$\text{Fe}_{16}\text{O}_{16}(\text{OH})_{12}(\text{SO}_4)_2$	277
Sicklerite	$\text{Li}(\text{Mn},\text{Fe}^{2+})\text{PO}_4$	170
Tinticite*	$\text{Fe}_4(\text{PO}_4)_3(\text{OH})_3 \cdot 5\text{H}_2\text{O}$	192
Triphylite	$\text{LiFe}^{2+}\text{PO}_4$	170

* Theoretical capacities were calculated from dehydrated-type compounds. ⁺Since Mn is an active species and the formula is not fixed, the exact theoretical capacity is not included. Minerals with Fe^{2+} are indicated in the chemical formula.

II. Experimental

1. Sample Preparation

The five minerals in Table 2 were purchased from The Netherlands Rock (Goudse Steen 15, 3961XS Wijk bij Duurstede). Prior to using them, we first thoroughly ground the as-received minerals with mortar and pestle and then sieved

Table 2. Origin of minerals used in this work.

Mineral name	Origin, properties, and prices
Chalcophanite	Durango, Mexico, shiny black and spherical aggregates on matrix 9 cm×12 cm, Euro 25.00.
Diadochite	Belgium, gray-white earthy nodules, 3.5 cm×5 cm, Euro 6.50.
Laihuite	Colorado, Part of the oxidized portion of fayalite, 4.5 cm×6 cm, Euro 13.50.
Schwertmannite	Czech Republic, red powdery, numerous small pieces in a micromount box, Euro 13.00.
Tinticite	Indonesia, small white nodules in clay matrix, 3 cm×4 cm, Euro 12.00.

them using a mesh (No. 200, 75 μm).

2. Sample Characterization

To identify the crystal phase, we analyzed the crushed minerals by X-ray diffraction (XRD) using a MAC science MXP3A-HF diffractometer applying $\text{Cu-K}\alpha$ radiation. The scan data were collected in the 2θ range of 10–60 degrees. We obtained the powder morphology by a scanning electron microscopy (SEM, Hitachi S-800) and performed the thermogravimetric-differential thermal analysis (TG-DTA) using an SDT 2960 Simultaneous TG-DGA (TA instruments) at a heating rate of 10 $^\circ\text{C}/\text{min}$ in air.

3. Electrochemical Characterization

We performed charge/discharge tests in a SwagelockTM cell with a lithium foil counter electrode (FMC, Lithium Div.). The 30 mg of cathode pellet, consisting of 75% mineral, 20% super P carbon black, and 5% polytetrafluoroethylene, was pressed and then dried at 120 $^\circ\text{C}$ for 2 hours in a vacuum oven. The electrolyte used was 1mol LiPF_6 in a 1:1 ethylene carbonate/dimethyl carbonate solution. The entire process was carried out in an environmentally controlled dry room. We measured the electrochemical properties with a Biologic MacPile II charge/discharge cyler at a voltage window of 4.3 to 1.0 V. The cyclic voltammetric measurement was conducted at a scan rate of 30 $\mu\text{V}/\text{s}$.

III. Results and Discussion

1. Discharge Behavior of Iron-Containing Minerals

Figure 1 shows the 1st discharge curves of the five minerals at a constant specific current of 10 mA/g. In this cycle, we

observed that most of the minerals showed large reduction peaks centered at below 2.0 V. For example, schwertmannite showed a large capacity of about 500 mAh/g, exceeding its theoretical capacity of 277 mAh/g. This means that it was over-lithiated at a low voltage of 1.5 V, giving rise to metallic iron. Interestingly, the diadochite exhibited two reduction peaks centered at 3.0 V and 1.05 V. This indicates that diadochite can be used as a cathode material. With this result, we intensively carried out further experiments on the mineral diadochite.

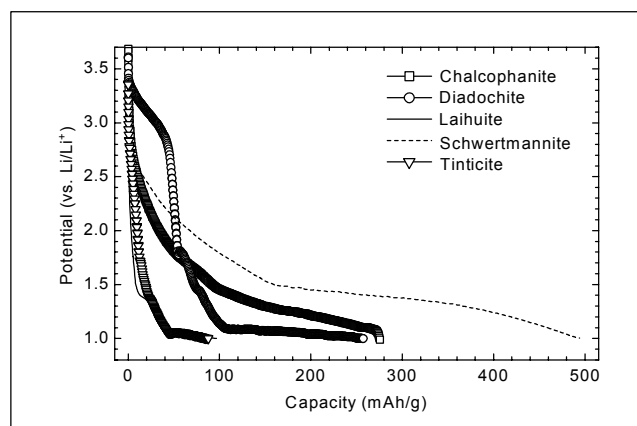


Fig. 1. Discharge profiles of five minerals. The cutoff potential was 1.0 V.

2. Characterization of Diadochite

Figure 2 shows the TG-DTA curves of diadochite $\text{Fe}_2\text{PO}_4\text{SO}_4\text{OH}\cdot 6\text{H}_2\text{O}$. We obtained four samples at 300, 500, 600, and 700 °C, which are assigned as DT300, DT500, DT600, and DT700. The two large endothermic peaks around 114 and 164 °C with a weight loss of 25% (below 250 °C) correspond to the evaporation of six water molecules (theoretical weight loss = 25%). Note that the weight continuously decreases up to 500 °C, which may be due to dehydroxylation. At 550 °C, the sulfur component had partly begun to evaporate and completely decomposed at 650 °C. We confirmed this by elemental analysis (Table 3). This indicates that diadochite is decomposed as follows: $\text{Fe}_2\text{PO}_4\text{SO}_4\text{OH}\cdot 6\text{H}_2\text{O} \rightarrow \text{Fe}_2\text{PO}_4\text{SO}_4\text{OH} + 6\text{H}_2\text{O} (\uparrow) \rightarrow \text{FePO}_4 + 0.5\text{Fe}_2\text{O}_3 + 0.5\text{H}_2\text{O} (\uparrow) + \text{SO}_3 (\uparrow)$. In fact, the dehydrated diadochite $\text{Fe}_2\text{PO}_4\text{SO}_4\text{OH}$ has a composition similar to dehydrated phosphosiderite FePO_4 [10] or $\text{LiFe}_2\text{PO}_4(\text{SO}_4)_2$ [14]. The positive charge due to the SO_4^{2-} in the $\text{Fe}_2\text{PO}_4\text{SO}_4\text{OH}$ is balanced by the OH^- group, while the negative charge in the $\text{LiFe}_2\text{PO}_4(\text{SO}_4)_2$ is compensated for by the Li^+ .

Figure 3 shows the XRD patterns of the samples prepared at different temperatures. The pristine diadochite was identified to a triclinic phase corresponding to JCPDS-ICDD No. 42-1364 ($a=9.584\text{Å}$, $b=9.748\text{Å}$, $c=7.338\text{Å}$, $\alpha=98.78^\circ$, $\beta=108.0^\circ$,

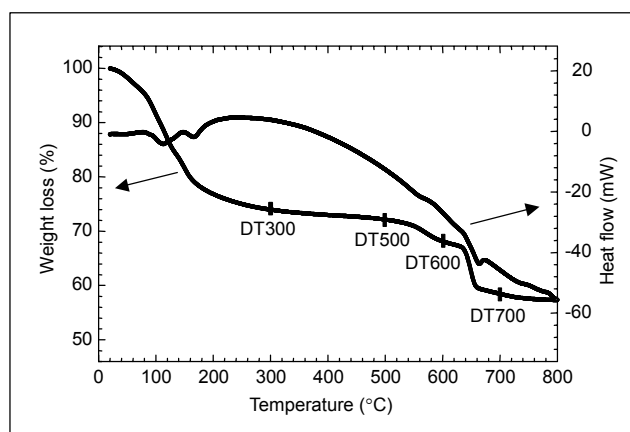


Fig. 2. TG-DTA curves of diadochite at a heating rate of 10 °C/min.

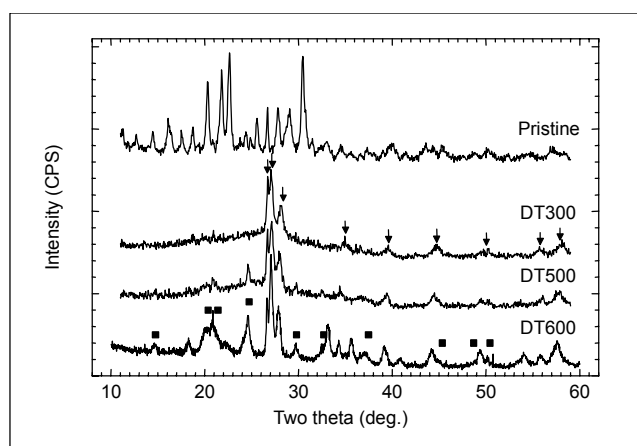


Fig. 3. XRD patterns of the samples prepared at different temperatures. ■: Fe_2O_3 , †: unknown phase.

Table 3. Elemental analysis of four samples.

Sample	DT300	DT500	DT600	DT700
S content (%)	9.6±0.1	9.1±0.1	5.4±0.1	0.4±0.1

$\gamma=63.869^\circ$). DT300 is completely different from the diadochite and similar to $\text{FeFe}_2(\text{PO}_4)_2(\text{OH})_2$ (JCPDS-ICDD No. 33-0668), but we have not yet explored the crystal structure. The XRD pattern of DT600 showed that the diffraction peaks of Fe_2O_3 , due to decomposition as revealed in the TG-DTA curves, was well developed with an unknown phase.

3. Electrochemical Behavior of Diadochite

We carried out investigations of the lithium reactivity with diadochite on three samples. Figures 4 and 5 show the initial five discharge/charge cycles and discharge capacities. For all

samples, the large capacity differences between the 1st and 2nd discharge are evident. It has been reported that the discharge capacity of an olivine LiFePO_4 electrode is limited by the diffusion rate of the lithium ions in the LiFePO_4 particles. In this respect, the discharge capacity may not be greatly improved, because DT300 powders are arranged in about $50 \mu\text{m}$ sized aggregates of crystallites that are between 1 and $5 \mu\text{m}$ (Fig. 6). Note that the capacities of DT500 are higher than those of DT300. The reason for such a result is unclear, but it seems to be due to the contribution of an Fe_2O_3 phase as the discharge profile for DT600 suggests. Actually, the color of the pristine diadochite turned from whitish gray to brown as the heating temperature increased.

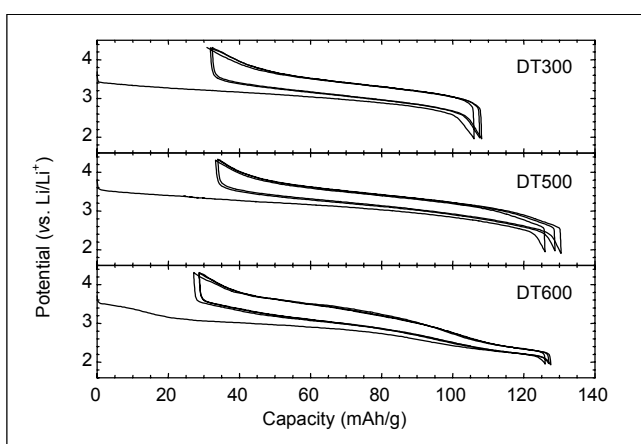


Fig. 4. Charge/discharge profiles of the samples at a specific current of 10mA/g at $4.3\text{--}2.0\text{ V}$.

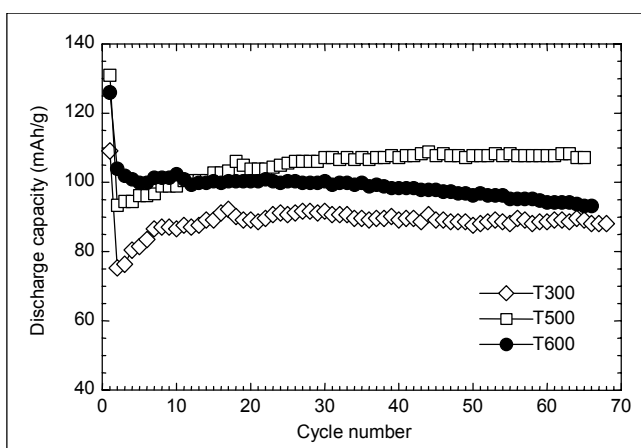


Fig. 5. Discharge capacities of three samples.

To see the electrochemical properties of DT300 at a low potential, we applied the potential down to 1.25 V (Fig. 7). We considered it of particular significance that the cell could be cycled with surprisingly good cyclability, leading to a 2nd discharge capacity of above 300 mAh/g . It exhibited a new



Fig. 6. SEM photograph of DT300.

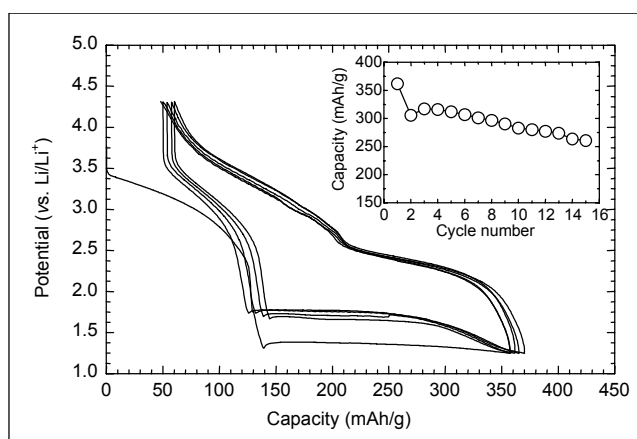


Fig. 7. Charge/discharge profiles of DT300 at a voltage range of 4.3 to 1.25 V .

plateau of 1.3 V at the 1st discharge and 1.7 V at the 2nd cycle. Johnson et al. observed a similar low-voltage electrochemical behavior with the charge/discharge profile of an $\text{Li/Li}(\text{Mn}_{0.46}\text{Ni}_{0.46}\text{Ti}_{0.05}\text{Li}_{0.02})\text{O}_2$ cell [15]. In this case, the electrochemical reaction was hypothesized to form $\text{Li}_2(\text{Mn}_{0.46}\text{Ni}_{0.46}\text{Ti}_{0.05}\text{Li}_{0.02})\text{O}_2$, which is isostructural with Li_2MnO_2 and Li_2NiO_2 , where there are two oxidation states of Mn and Ni. In the diadochite, we can imagine two possibilities on lithium insertion. One is the reduction of Fe^{3+} to Fe^+ , the other is the reduction of Fe^{3+} as metallic Fe. Since Fe^+ is very unstable, the former is unrealistic. If the latter is true, it is quite interesting phenomena on the point that the two plateaus are easily reversible, even though the DT300 at 1.25 V (about $\text{Li}_4\text{Fe}_2\text{PO}_4\text{SO}_4\text{OH}$) changes into an amorphous phase (not shown here).

Figure 8 shows the current-voltage curves obtained over the initial five cycles. In the 1st, we observed three peaks centered

at 3.0 V, 1.8 V, and 1.3 V for the first anodic scan and two peaks at 3.0 V and 1.5 V for the subsequent scans. This indicates that an irreversible structural transformation from the crystalline form of DT300 to an amorphous phase had certainly taken place during the first discharge cycle. The structure of the lithiated $\text{Li}_x\text{Fe}_2\text{PO}_4\text{SO}_4\text{OH}$ phase at the end of the 1st discharge cycle was completely different from that of DT300.

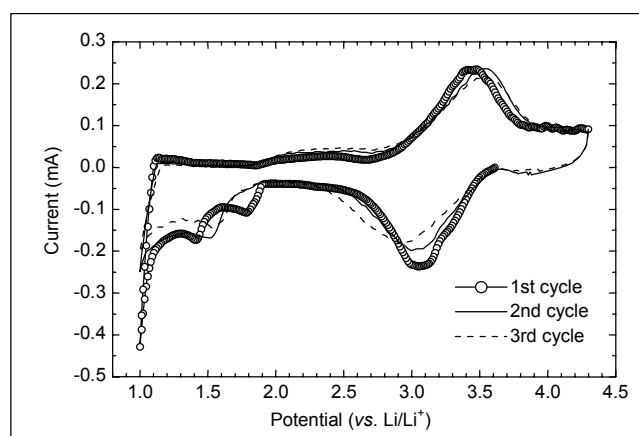


Fig. 8. Current vs. potential curves of DT300 at a voltage range of 4.3 to 1.0 V.

IV. Conclusions

The present work describes for the first time the electrochemical properties of the mineral diadochite, which we obtained by heat-treating pristine $\text{Fe}_2\text{PO}_4\text{SO}_4\text{OH}\cdot 6\text{H}_2\text{O}$. In both capacity and cyclability, the heat-treated diadochite was better than the $\text{LiFe}_2\text{PO}_4(\text{SO}_4)_2$. In parallel with the widely investigated olivine LiFePO_4 and its related phases, diadochite can be classified as a new 3 V cathode material for lithium ion rechargeable batteries. One of the most encouraging advantages is that diadochite is readily obtained in nature while the olivine LiFePO_4 must be prepared in a reducing atmosphere. Additionally, the various compositions of the $\text{FePO}_4\text{-SO}_4\text{-OH}$ system deserve to be studied in more detail.

References

[1] E. Baudrin, S. Laruelle, S. Denis, M. Touboul, and J.-M. Tarascon, "Synthesis and Electrochemical Properties of Cobalt Vanadates vs. Lithium," *Solid State Ionics*, vol. 123, no.1-4, Aug. 1999, pp. 139-153.
 [2] Y. Idota, T. Kudota, A. Matsufuji, A. Maekawa, and T. Miyasaka, "Tin-Based Amorphous Oxide: A High-Capacity Lithium-Ion-Storage Material," *Science*, vol. 276, May 1997, pp. 1394-1397.
 [3] O. Mao, R.L. Turner, I.A. Courtney, B.D. Fredericksen, M.I. Buckett, L.J. Krause, and J.R. Dahn, "Active/Inactive Nanocomposites as Anodes for Li-Ion Batteries," *Electrochem.*

Solid State Lett., vol 2, no. 1, Jan. 1999, pp. 3-5.

[4] M. Nishijima, T. Kagohashi, M. Imanishi, Y. Takeda, O. Yamamoto, and S. Kondo, "Synthesis and Electrochemical Studies of a New Anode Material, $\text{Li}_{3-x}\text{Co}_x\text{N}$," *Solid State Ionics*, vol. 83, no. 1-2, Jan. 1996, pp. 107-111.
 [5] P. Poizot, S. Laruelle, S. Grugeon, L. Dupont, and J.-M. Tarascon, "Nano-Sized Transition-Metal Oxides as Negative-Electrode Material for Lithium-Ion Batteries," *Nature*, vol. 407, 2000, pp. 496-499.
 [6] A.K. Padhi, K.S. Nanjundaswamy, and J.B. Goodenough, "Phospho-Olivines as Positive-Electrode Materials for Rechargeable Lithium Batteries," *J. Electrochem. Soc.*, vol. 144, no.4, Apr.1997, pp. 1188-1194.
 [7] S.-Y. Chung, J.T. Bloking, and Y.-M. Chiang, "Electronically Conductive Phospho-Olivines as Lithium Storage Electrodes," *Nature Materials*, vol. 1, Oct. 2002, pp. 123-128.
 [8] N. Ravet, Y. Chouinard, J.F. Magnan, S. Besner, M. Gauthier, and M. Armand, "Electroactivity of Natural and Synthetic Triphylite" *J. Power Sources*, vol. 97-98, July 2001, pp. 503-507.
 [9] S. Whittingham, S. Yang, Y. Song, K. Ngala, and P. Y Zavalij, "Layered Cathode Materials", *11th Int'l Meeting on Lithium Batteries*, 2002, p. 207.
 [10] C. Masquelier, P. Reale, C. Wurm, M. Morecrette, L. Dupont, and D. Larcher, "Hydrated Iron Phosphates $\text{FePO}_4\cdot n\text{H}_2\text{O}$ and $\text{Fe}_4(\text{P}_2\text{O}_7)_3\cdot n\text{H}_2\text{O}$ as 3 V Positive Electrodes in Rechargeable Li Batteries", *J. Electrochem. Soc.*, vol. 148, no. 9, 2002, pp. A1037-A1044.
 [11] J.L.C. Rowsell, J. Gaubicher, and L.F. Nazar, "A New Class of Materials for Lithium-Ion Batteries: Iron(III) Borates," *J. Power Sources*, vol. 97-98, July 2001, pp. 254-257.
 [12] J.L.C. Rowsell and L.F. Nazar, "Synthesis, Structure, and Solid-State Electrochemical Properties of Cr_3BO_6 : a New Chromium(III) Borate with the Norbergite Structure," *J. Mater. Chem.*, vol. 11, no. 12, Dec. 2001, pp. 3228-3233.
 [13] Y.-S. Hong, K. S. Ryu, Y. J. Park, M. G. Kim, J. M. Lee, and S. H. Chang, "Amorphous FePO_4 as 3 V Cathode Material for Lithium Secondary Batteries", *J. Mater. Chem.*, vol.12, 2002, pp. 1870-1874.
 [14] J.B. Goodenough et al., *Cathode materials for secondary rechargeable lithium batteries*, US Patent, 5,910,382, to Board of Regents, University of Texas Systems, Austin, Texas, 1999.
 [15] C.S. Johnson, J.-S. Kim, A.J. Kropf, A.J. Kahaian, J.T. Vaughey, and M.M. Thackeray, "The Role of Li_2MO_2 Structures (M=metal ion) in the Electrochemistry of $(x)\text{LiMn}_{0.5}\text{Ni}_{0.5}\text{O}_2\cdot(1-x)\text{Li}_2\text{TiO}_3$ Electrodes for Lithium-Ion Batteries", *Electrochem. Commun.*, vol.4, 2002, pp. 492-498.



Young-Sik Hong received the MS and the PhD degrees in chemistry from Korea University in Seoul, Korea, in 1992 and 1997. From Oct. 1997 to Sept. 1999, he was a Postdoc at the Institut de Chimie de la Matière Condensée de Bordeaux (ICMCB), at Bordeaux University in France. He studied the synthesis and

characterization of inorganic solid compounds using an X-ray diffractometer. From Oct. 1999 to Feb. 2001, he worked at Korea University in Seoul, Korea, as a Research Assistant Professor where he was engaged in research on lithium secondary batteries. In Mar. 2001, he moved to the Basic Communication Research Laboratory at the Electronic and Telecommunications Research Institute (ETRI) in Daejeon, Korea, where he has continued his research on the development of cathode materials for lithium secondary batteries.



Kwang Sun Ryu received the BS and MS degrees in chemistry from Yonsei University in Seoul, Korea in 1986 and 1990 and his PhD degree in polymer physical chemistry from Yonsei University in 1996. From 1996 to 1997, he was a Postdoctoral Researcher in ETRI and Tokyo University of Arg. & Tech (TUAT).

Since 1998, he has been with the Research Department in ETRI and worked in the Power Source Device Team. His current topics of interest are conducting polymers, polymer physical properties, nano-polymer technology, lithium secondary batteries, supercapacitors, and new concept power source devices.



Soon Ho Chang received the BS and MS degrees in chemistry from Yonsei University in Korea in 1982 and the PhD degree for research in intercalation/deintercalation in inorganic compounds from Bordeaux University in France in 1989. From 1990 to 2001, he was with Research Department in ETRI and worked

in the Power Source Device Team. Since 2002, he has been in charge of the Applied Device Department at the Basic Communication Research Laboratory of ETRI.